

Supplementary Information

**Sustainable wastewater treatment and recycle in membrane manufacturing**

*Mayamin Razali<sup>1,§</sup>, Jeong F. Kim<sup>2,§</sup>, Martin Attfield<sup>3</sup>, Peter Budd<sup>3</sup>, Enrico Drioli<sup>2,4</sup>, Young Moo Lee<sup>2</sup>,  
Gyorgy Szekely<sup>1,\*</sup>*

<sup>1</sup>. School of Chemical Engineering & Analytical Science, The University of Manchester, The Mill, Sackville Street, Manchester M13 9PL, United Kingdom

<sup>2</sup>. WCU Department of Energy Engineering, Hanyang University, Republic of Korea

<sup>3</sup>. School of Chemistry, The University of Manchester, United Kingdom

<sup>4</sup>. Institute on Membrane Technology (ITM-CNR), Via P. Bucci 17/C, I-87030 Rende, CS, Italy

<sup>§</sup> Authors contributed equally

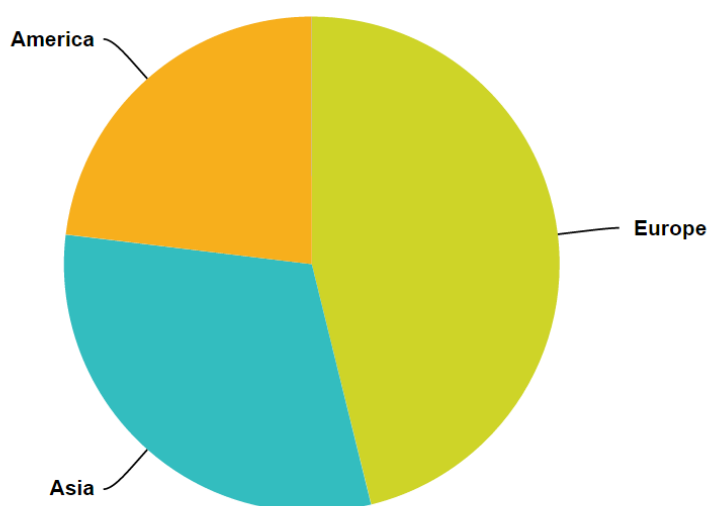
<sup>\*</sup> Corresponding author: +44 (0) 161 306 4366, [gyorgy.szekely@manchester.ac.uk](mailto:gyorgy.szekely@manchester.ac.uk)

## Table of Contents

1. Survey on wastewater in the Membrane Industry	S3
2. Adsorbent screening	S6
3. Adsorption isotherm parameters	S7
3.1. Adsorption Isotherm	S7
3.2. Kinetic Isotherm	S11
4. Adsorbent regeneration	S13
5. Continuous water purification	S14
6. Preparation and characterisation of metal-organic frameworks	S15
7. Characterization of PIM-1	S19
8. Preparation and characterization of imprinted polymers	S20
9. Solvent flux decline of the membranes	S23
10. Calculation of Membrane Wastewater Generation	S24
11. Sustainability Assessment of Wastewater Treatment Process	S25
11.1. Calculation of adsorbent mass	S25
11.2. Calculation of Process Mass Intensity	S25
11.3. Adsorbent Recovery Calculation	S26
11.4. Process Energy Calculation	S27
References	S28

## 1. Survey on wastewater in the Membrane Industry

List of companies who were contacted to fill out the survey: Lenntech, Pall, Evonik, SolSep, Novamem, Membrane Hitec, Borsig, Koch, Millipore, Dow, Permionics Membranes, Microdyn-Nadir, GE Healthcare Life Sciences, PCA Gmbh, Fraunhofer, Baker Manufacturing Co, Econity, Pure EnviTech, Evoqua, Hydro Treat Technologies, SeptraTek, Deerfos America Inc, Synopex. Out of 23 companies contacted 13 responses were received.



Answer Choices	Responses	
Europe	46.15%	6
Asia	30.77%	4
America	23.08%	3
Australia	0.00%	0
Total		13

Figure S1. Survey Question 1. Where is your company located?

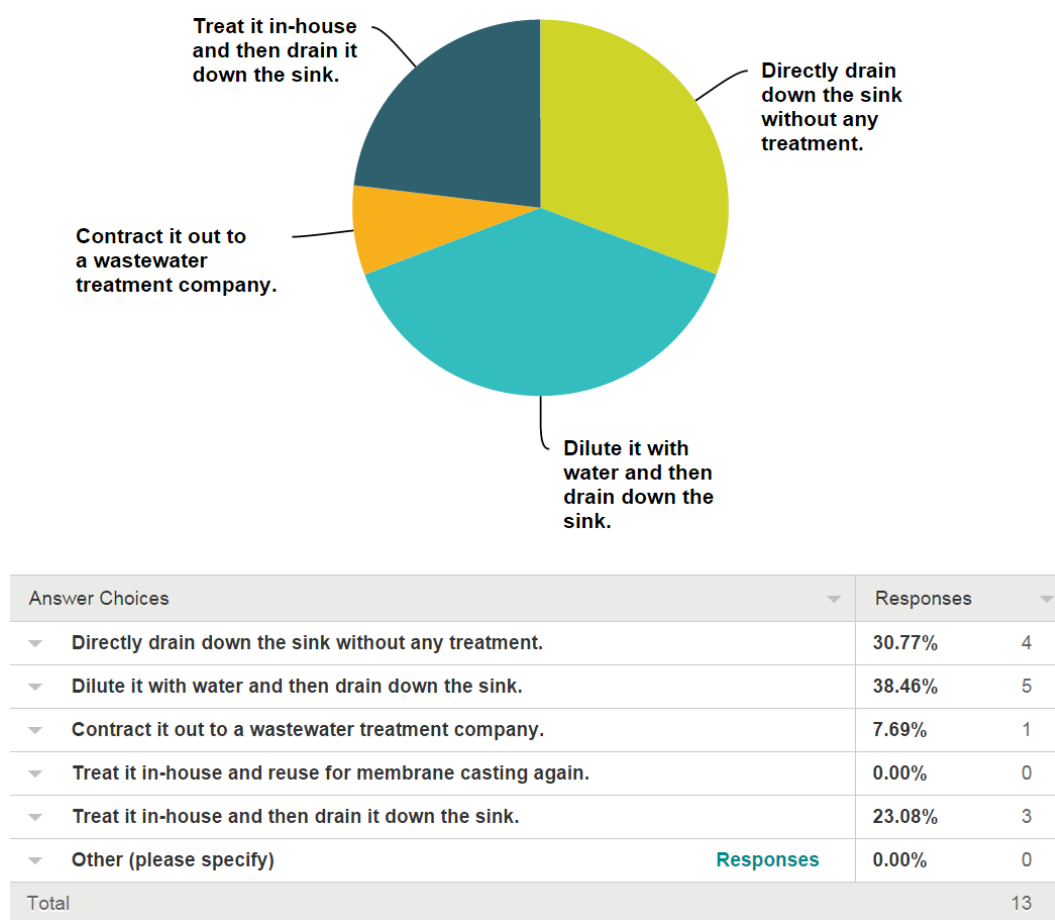


Figure S2. Survey Question 2. How do you dispose of your wastewater resulting from the coagulation bath?

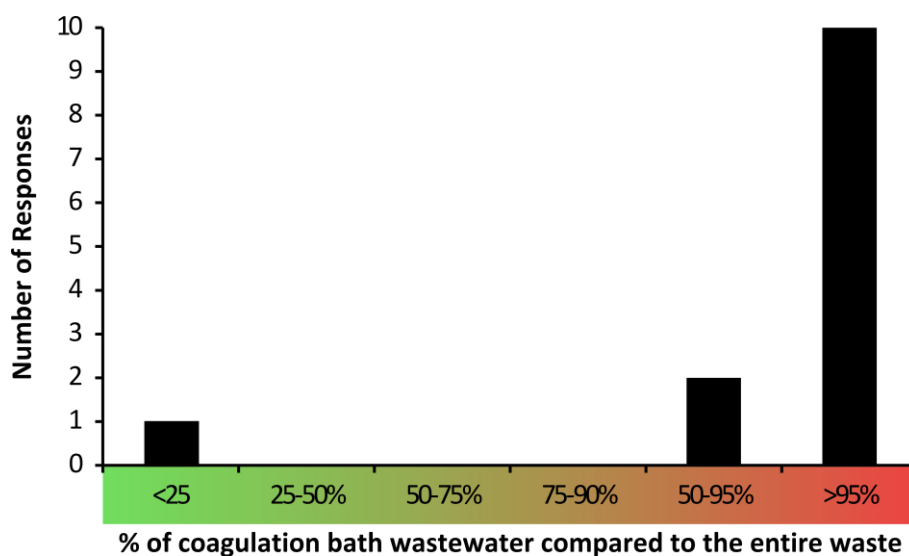


Figure S3. Survey Question 3. What is the % of wastewater resulting from coagulation bath compared to the entire waste generated during the membrane fabrication process?

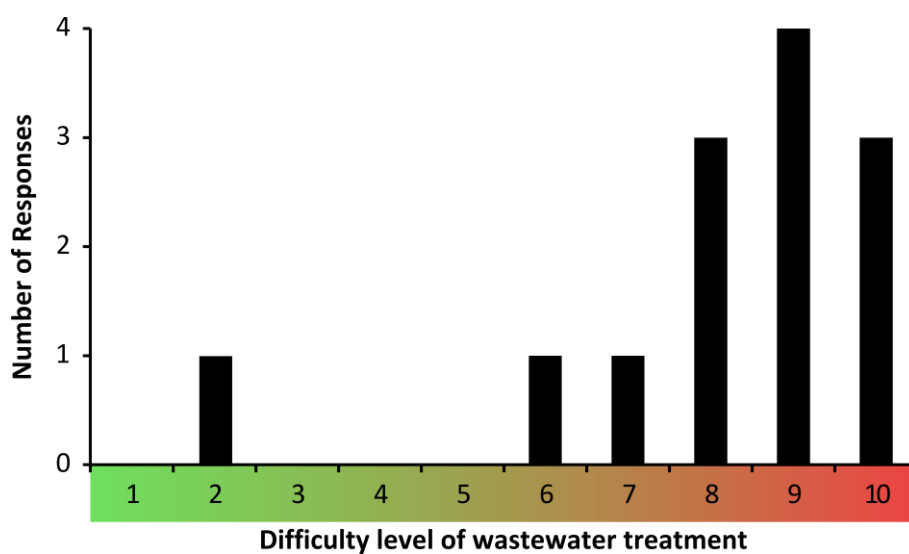


Figure S4. Survey Question 4. Using a scale 0 - 10 (very easy to very difficult), How difficult is it to dispose your coagulation wastewater?

## 2. Adsorbent screening

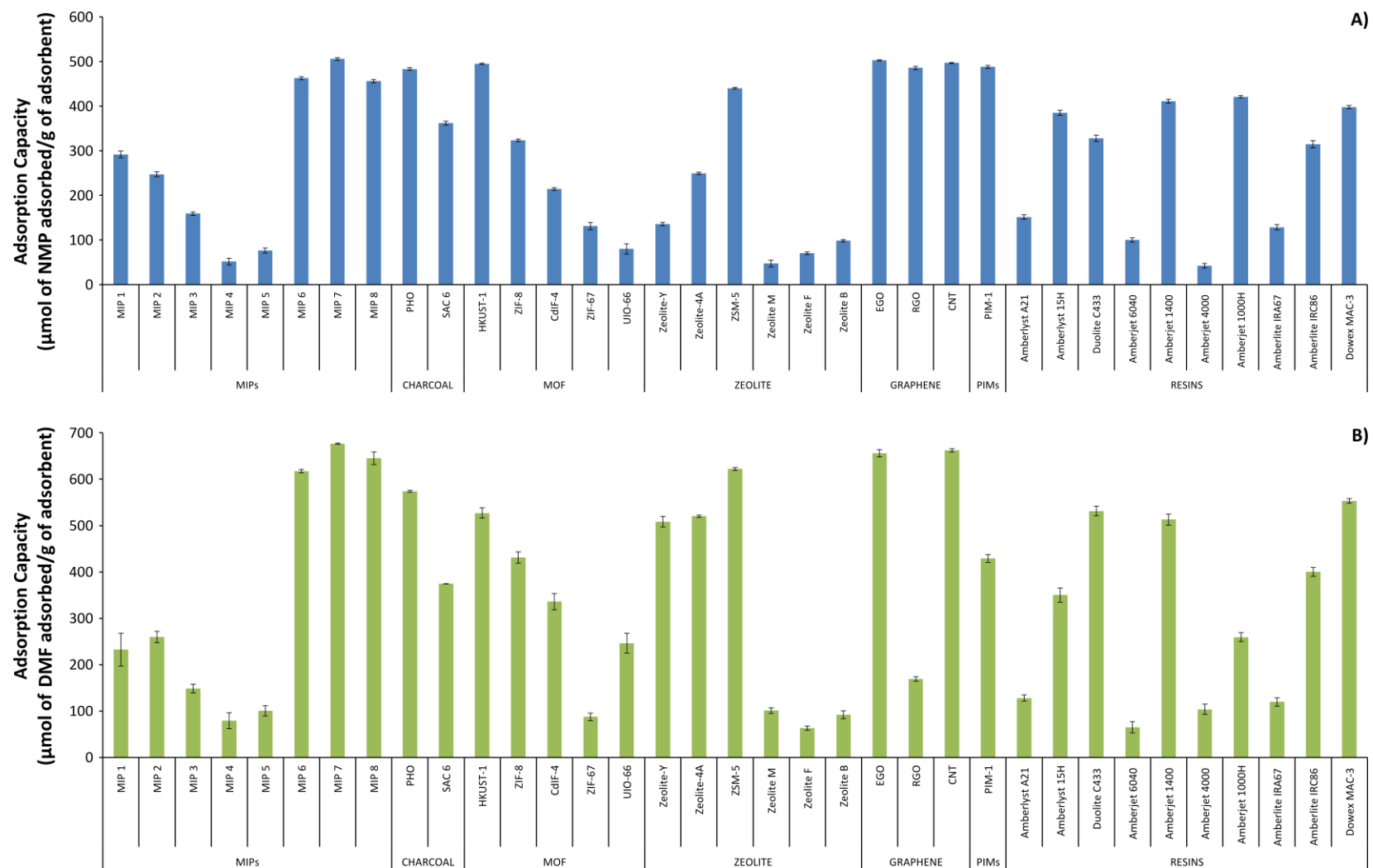


Figure S5. Adsorption capacity of all adsorbents from the seven classes of materials investigated. Panel A) shows the adsorption of NMP whilst panel B) shows the adsorption of DMF. The adsorbent mass to system volume ratio was fixed at 20 g.L<sup>-1</sup>.

### 3. Adsorption isotherm and kinetic parameters

#### 3.1. Adsorption Isotherm

Linear isotherm is the simplest adsorption equation and it follows Henry's Law for gases. The equation for this model as below, with  $a_L$  and  $b_L$  represents Linear isotherm constants. Linear isotherm model is denoted as in Eq. S1.

$$q_e = a_L + b_L C_e \quad \text{Eq. S1.}$$

Langmuir isotherm is one of the classic models that have been used frequently in adsorption studies. Langmuir equation based on three assumptions. First the surface is homogeneous or the adsorption energy or active site is constant in the entire sites. Second each site can only accommodate one molecule or one atom. Third adsorption on surface is localised, which molecules or atoms are adsorbed at definite, localised site. At low adsorbate concentration, it reduces to linear isotherm and follow Henry's Law. At high adsorbate concentration, it predicts monolayer adsorption. This model is expressed by Equation S2 with  $N$  is homogeneous binding site density ( $\text{mg.g}^{-1}$ ) and  $K_L$  is Langmuir constant or also known as rate of adsorption and adsorption constant ( $\text{L.mg}^{-1}$ ).

$$q_e = \frac{N K_L C_e}{1 + K_L C_e} \quad \text{Eq. S2.}$$

Freundlich isotherm is also one of the classic models that have been used frequently in adsorption studies, beside Langmuir. Freundlich isotherm has been used to compensate limitation from Langmuir model. Freundlich isotherm model can be applied for multilayer adsorption and heterogeneous; reversible and non-ideal adsorption process. Freundlich isotherm will give more accurate for approximation at lower concentrations. This isotherm model is expressed by Equation S3, with  $K_F$  is the Freundlich constant ( $\text{L.mg}^{-1}$ ) and  $n_F$  is heterogeneity index. If the value of  $n_F$  is in between of 1 to 10, the binding sites are heterogeneous and adsorption process can be modelled by Freundlich isotherm model.

$$q_e = K_F (C_e)^{1/n_F} \quad \text{Eq. S3.}$$

Freundlich Extended Isotherm model is the extension of Freundlich isotherm model, which match for multilayer and heterogeneous adsorption. This model is expressed by the following equation with  $K_{FE}$  is Freundlich Extended constant ( $\text{L.g}^{-1}$ ) and  $n_{FE}$  is Heterogeneity index. Freundlich Extended Isotherm model is denoted as in Eq. S4.

$$q_e = K_{FE} (1 + C_e)^{1/n_{FE}} \quad \text{Eq. S4.}$$

Reciprocal adsorption isotherm is denoted as in Eq. S5. with  $a_R$  and  $b_R$  are the constants, where the constant  $b_R$  shows the adsorption power.

$$q_e = \frac{1}{a_R + b_R C_e} \quad \text{Eq. S5.}$$

Sips isotherm model is combination of Langmuir and Freundlich isotherm model. Sips isotherm model compensates the limitation in Langmuir and Freundlich model. Sips isotherm model can be applied for both homogeneous and heterogeneous adsorption at either high or low concentrations. At low concentration, it effectively reduces to a Freundlich isotherm. Meanwhile at high concentration, it predicts a monolayer sorption capacity characteristic of the Langmuir isotherm. This model is expressed by Equation S6 with  $K_L$  is Langmuir constant ( $\text{L.mg}^{-1}$ ),  $N$  is binding site density ( $\text{mg.g}^{-1}$ ) and  $n$  is Heterogeneity index.

$$q_e = \frac{N K_L C_e^n}{1 + K_L C_e^n} \quad \text{Eq. S6.}$$

Toth adsorption isotherm is improvement of Langmuir isotherm. This model favors heterogeneous adsorption at both low and high concentration. This model is expressed by the Equation S7 with  $K_T$ ,  $a_T$  and  $t$  are the constants.

$$q_e = \frac{K_T C_e}{(a_T + C_e)^{1/t}} \quad \text{Eq. S7.}$$

Redlich–Peterson is expressed by the following Equation S8 with  $K_R$ ,  $a_R$  and  $g$  are the constants. At high concentrations and as the exponent ( $g$ ) tend to zero, this model approach Freundlich model. At low concentration and as the exponent ( $g$ ) tends to one, this model approach Langmuir model.

$$q_e = \frac{K_R C_e}{1 + a_R C_e^g} \quad \text{Eq. S8.}$$

Jovanovic isotherm model considers 2 assumptions from Langmuir model, which are adsorption occur in monolayer and surface of binding sites are equal. Differ from Langmuir model, this model also assumes there are interaction between adsorbed template and free template. Existence of interaction between adsorbed and free template will increase the rate of adsorption or adsorption constant,  $K_j$  but decrease the binding site density,  $N_j$ . This model is expressed by Equation S9.

$$q_e = N_j (1 - e^{-K_j C_e}) \quad \text{Eq. S9.}$$



Table S1. Adsorption isotherm parameters

Isotherm Models	Parameters	Charcoal PHO		MIP MIP7		MOF HKUST-1		Zeolite ZSM-5		Graphene EGO	
		DMF	NMP	DMF	NMP	DMF	NMP	DMF	NMP	DMF	NMP
Linear	$a_L$	0.0001	0.0431	0.0525	0.0593	-0.0348	0.0413	0.0262	0.0285	0.0784	0.0973
	$b_L$	0.0207	0.0001	0.0001	0.0003	0.0003	0.0002	0.0002	0.0001	0.0000	0.0001
	$R^2$	<b>0.9693</b>	<b>0.7181</b>	<b>0.6692</b>	<b>0.7733</b>	<b>0.9205</b>	<b>0.9172</b>	<b>0.9872</b>	<b>0.9546</b>	<b>0.2302</b>	<b>0.6130</b>
Langmuir	N	0.1120	0.1107	0.1452	0.2255	-0.3156	0.1716	0.2027	0.1607	0.0843	0.1519
	$K_L$	0.0033	0.0181	0.0409	0.0211	-0.0005	0.0114	0.0030	0.0034	0.7880	0.1010
	$R^2$	<b>0.9103</b>	<b>0.9918</b>	<b>0.9759</b>	<b>0.9793</b>	<b>0.2846</b>	<b>0.9462</b>	<b>0.9402</b>	<b>0.9872</b>	<b>0.9996</b>	<b>0.9999</b>
Freundlich	$K_F$	0.0779	0.1360	0.1931	0.1947	0.0198	0.1510	0.0813	0.0801	0.3024	0.2935
	$n_F$	1.9724	2.7270	3.4507	2.8810	0.9027	2.6330	1.7253	1.7931	21.5983	6.4475
	$R^2$	<b>0.9830</b>	<b>0.9271</b>	<b>0.9619</b>	<b>0.9811</b>	<b>0.8947</b>	<b>0.9699</b>	<b>0.9956</b>	<b>0.9858</b>	<b>0.5456</b>	<b>0.9412</b>
Extended Freundlich	$K_{FE}$	0.0028	0.0099	0.0196	0.1947	0.0001	0.0122	0.0030	0.0029	0.0636	0.0580
	$n_{FE}$	1.9616	2.6983	3.1686	2.8810	0.8979	2.5780	1.7123	1.7825	21.459	6.2814
	$R^2$	<b>0.9829</b>	<b>0.9251</b>	<b>0.9666</b>	<b>0.9811</b>	<b>0.8956</b>	<b>0.9682</b>	<b>0.9954</b>	<b>0.9854</b>	<b>0.5421</b>	<b>0.9339</b>
Reciprocal	$a_R$	38.676	27.679	25.277	23.627	43.557	26.764	31.130	31.8710	12.8780	10.7980
	$b_R$	-0.0380	-0.0261	-0.0293	-0.0331	-0.0620	-0.0316	-0.0362	-0.0334	-0.0016	-0.0076
	$R^2$	<b>0.7881</b>	<b>0.5509</b>	<b>0.5171</b>	<b>0.4683</b>	<b>0.8871</b>	<b>0.6048</b>	<b>0.7142</b>	<b>0.6924</b>	<b>0.2472</b>	<b>0.4882</b>

Continuation of *Table S1*.

<b>Sips</b>	N	56.501	0.1123	0.2373	0.4791	3.1406	16.5080	28.2843	0.2633	0.1817	0.1341
	K <sub>L</sub>	0.0000	0.0126	0.0733	0.0387	0.0000	0.0008	0.0001	0.0065	0.5711	0.0111
	n	1.0074	1.0666	0.4795	0.4721	1.9076	0.3807	0.5930	0.7243	0.0000	1.0842
	<b>R<sup>2</sup></b>	<b>0.9120</b>	<b>0.9271</b>	<b>0.9619</b>	<b>0.9811</b>	<b>0.8947</b>	<b>0.9699</b>	<b>0.9956</b>	<b>0.9858</b>	<b>0.9025</b>	<b>0.3563</b>
<b>Toth</b>	k <sub>T</sub>	0.0005	0.2161	0.0259	0.0261	0.0003	0.0136	0.0029	0.0038	0.1233	0.1467
	a <sub>T</sub>	17944	88.577	0.2992	0.3679	35023	0.7085	0.0000	0.9304	6.2465	68.915
	t	9.1307	0.9163	1.3695	1.4887	230510	1.5913	2.4442	2.0677	1.0821	0.9904
	<b>R<sup>2</sup></b>	<b>0.9120</b>	<b>0.9271</b>	<b>0.9619</b>	<b>0.9811</b>	<b>0.8947</b>	<b>0.9699</b>	<b>0.9956</b>	<b>0.9858</b>	<b>0.9025</b>	<b>0.3563</b>
<b>Redlich Peterson</b>	K <sub>R</sub>	0.0002	0.0016	0.0424	0.0579	0.0012	0.0427	0.4997	0.0099	0.1771	0.0577
	a <sub>R</sub>	0.0480	0.0098	1.4294	2.0166	3.3108	3.0180	172.7334	2.3540	2.1976	2.2828
	g	0.0000	1.0534	0.7510	0.6863	0.0000	0.6341	0.4093	0.4956	0.8543	0.7479
	<b>R<sup>2</sup></b>	<b>0.1364</b>	<b>0.9816</b>	<b>0.9809</b>	<b>0.9884</b>	<b>0.0746</b>	<b>0.9887</b>	<b>0.9916</b>	<b>0.9783</b>	<b>0.9926</b>	<b>0.9923</b>
<b>Jovanovic</b>	N <sub>j</sub>	6.8552	0.1025	0.1482	0.2164	53.6871	0.1558	0.1717	0.1224	0.1827	0.0999
	k <sub>j</sub>	0.0000	0.0130	0.0084	0.0071	0.0000	0.0054	0.0024	0.0037	0.0502	1.0000
	<b>R<sup>2</sup></b>	<b>0.8598</b>	<b>0.9678</b>	<b>0.9315</b>	<b>0.9745</b>	<b>0.9202</b>	<b>0.9293</b>	<b>0.9738</b>	<b>0.9811</b>	<b>0.2282</b>	<b>0.1520</b>

### 3.2. Kinetic Isotherm

Lagergren's pseudo first order model considers that external, internal diffusion and adsorption are lumped and summed together. Pseudo first order model requires initial guess of concentration of adsorbate on adsorbent at equilibrium,  $B_e$ . This kinetic model is expressed by the following Equation S10 with  $k_1$  ( $h^{-1}$ ) is the rate constant of first order model.

$$q_t = q_e(1 - e^{-k_1 t}) \quad \text{Eq. S10.}$$

Ho's second order model was introduced by Ho and McKay in 1998 and it's consider exchange of electrons between adsorbate and adsorbent, as rate-limit step of bond formation. Concentration of adsorbate on adsorbent at equilibrium can be calculated without any initial guess as required in Lagergren's model. This kinetic model is expressed by the following Equation S11 with  $k_2$  ( $g.mg^{-1}.h^{-1}$ ) rate constant of second order model.

$$q_t = \frac{q_e^2 k_2 t}{q_e k_2 t + 1} \quad \text{Eq. S11.}$$

Elovich model introduced in 1939 and used to model heterogeneous adsorption process and surfaces. This kinetic model is expressed by the following equation with  $\alpha$  and  $\beta$  are the initial adsorption rate and desorption constant during experiment, respectively. Elovich model is expressed by Equation S12.

$$q_t = \frac{\ln(\alpha \cdot \beta)}{\beta} + \frac{1}{\beta} \ln t \quad \text{Eq. S12.}$$

Weber-Morris intraparticle diffusion model is expressed by Equation S13 with  $k_d$  is rate constant of intraparticle diffusion model ( $mg.g^{-1}.h^{-0.5}$ )

$$q_t = k_d t^{0.5} \quad \text{Eq. S13.}$$

Table S2. Kinetic Isotherm Parameter

Kinetic Models	Parameter	NMP						DMF					
		Charcoal PHO	MIP MIP7	MOF HKUST-1	Zeolite ZSM-5	Graphene EGO	PIM PIM-1	Charcoal PHO	MIP MIP7	MOF HKUST-1	Zeolite ZSM-5	Graphene EGO	PIM PIM-1
Lagregen's Pseudo First Order	$k_1$	0.0919	0.1477	0.1573	0.0789	0.0029	0.0030	0.0348	0.1570	0.0626	0.0742	0.0036	0.0023
	$q_e$	0.0081	0.0079	0.0275	0.0308	0.9479	0.9716	0.0153	0.0105	0.0394	0.0188	0.9683	0.9782
	$R^2$	<b>0.4033</b>	<b>0.4960</b>	<b>0.8885</b>	<b>0.8575</b>	<b>0.4159</b>	<b>0.6506</b>	<b>0.2471</b>	<b>0.6435</b>	<b>0.8474</b>	<b>0.6911</b>	<b>0.6457</b>	<b>0.6408</b>
Ho's Pseudo Second Order	$k_2$	370.04	193.55	28.838	28.467	28.509	10.410	491.771	136.870	13.191	79.055	32.076	13.493
	$q_e$	0.0486	0.0497	0.0503	0.0450	0.1018	0.0865	0.0417	0.0498	0.0417	0.0459	0.0986	0.0659
	$h$	0.8728	0.4787	0.0731	0.0576	0.2952	0.0779	0.8548	0.3397	0.0229	0.1668	0.3118	0.0586
	$R^2$	<b>1.0000</b>	<b>0.9999</b>	<b>0.9987</b>	<b>0.9966</b>	<b>0.9995</b>	<b>0.9966</b>	<b>1.0000</b>	<b>0.9999</b>	<b>0.9911</b>	<b>0.9997</b>	<b>0.9996</b>	<b>0.9965</b>
Elovich	$\beta$	243.90	158.73	104.16	131.57	57.142	57.471	312.50	161.29	114.94	181.81	47.846	75.188
	$\alpha$	30.134	1.2641	0.0970	0.1099	0.3830	0.1070	79.869	1.4928	0.0350	1.3830	0.1126	0.0814
	$R^2$	<b>0.1554</b>	<b>0.3035</b>	<b>0.7124</b>	<b>0.6861</b>	<b>0.5793</b>	<b>0.8066</b>	<b>0.1472</b>	<b>0.4907</b>	<b>0.8795</b>	<b>0.7526</b>	<b>0.8298</b>	<b>0.8164</b>
Weber-Moris	$k_d$	0.0057	0.0070	0.0094	0.0079	0.0176	0.0170	0.0045	0.0062	0.0085	0.0053	0.0201	0.0129
	$R^2$	<b>0.3289</b>	<b>0.4147</b>	<b>0.7588</b>	<b>0.8222</b>	<b>0.6611</b>	<b>0.8662</b>	<b>0.3285</b>	<b>0.5407</b>	<b>0.9217</b>	<b>0.7755</b>	<b>0.8607</b>	<b>0.8581</b>

## 4. Adsorbent Regeneration

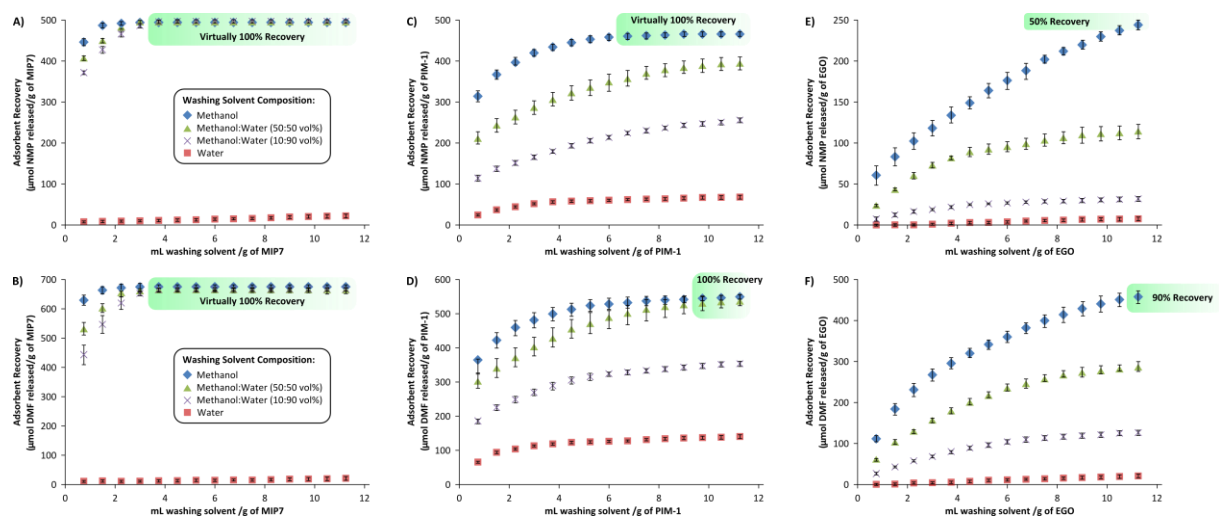


*Figure S6.* In search for the optimal regeneration of MIP7, PIM-1 and EGO adsorbents using washing solvents: water, methanol, methanol:water (50:50 vol%) and methanol:water (10:90 vol%).

## 5. Continuous water purification

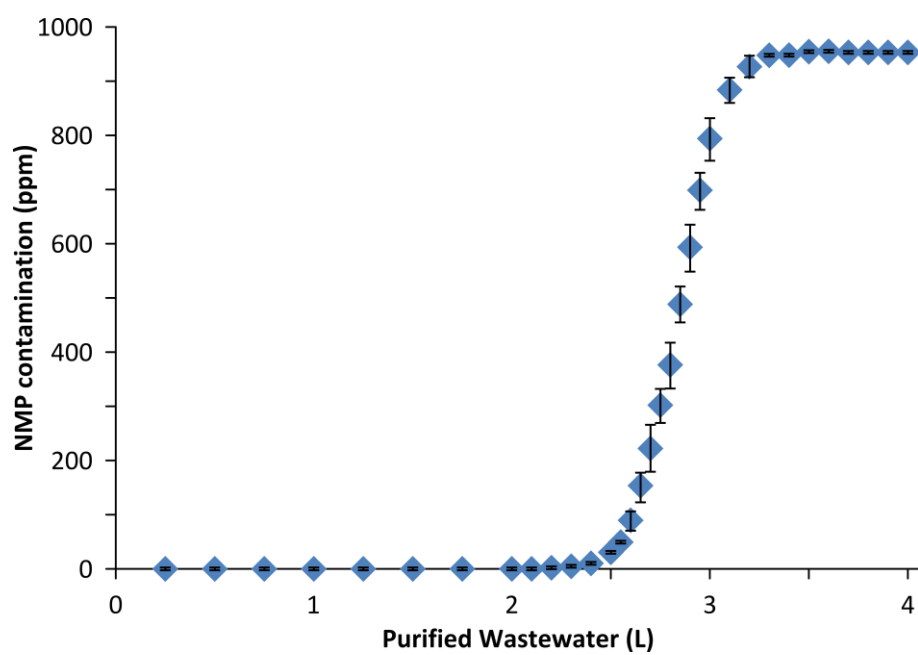


*Figure S7.* Breakthrough curve: NMP concentration at the adsorption column outlet as a function of processed volume wastewater, i.e. purified wastewater.

## 6. Preparation and characterisation of metal-organic frameworks

*HKUST-1* was synthesised by immersing two Cu foil electrodes ( $\sim 16 \text{ cm}^2$ ), approximately 2 cm apart, into a 1:1 ethanol:deionised water solution containing 48mM 1,3,5 – benzenetricarboxylic acid linker and 64mM methyltributylammonium methyl sulphate supporting electrolyte.<sup>1</sup> The solution was maintained at 55 °C and deaerated with  $\text{N}_2$  (g) whilst a PGSTAT302N potentiostat (Metrohm Autolab B.V., The Netherlands) was used to apply a fixed potential difference of 2.5 V between the two Cu foil electrodes for one hour. This generated HKUST-1 in solution which was collected by centrifugation. The HKUST-1 was then re-suspended in methanol, stirred and collected again by centrifugation before being left to dry.

*CdIF-4* crystals were synthesized by mixing  $\text{Cd}(\text{OAc})_2 \cdot 2\text{H}_2\text{O}$  (0.356 g) and 2-ethylimidazole (0.547 g) in a 20 ml scintillation vial, before adding 10 ml of n-butanol to the mixture.<sup>2</sup> The mixture was stirred for few minutes to dissolve the reactants. The scintillation vial was capped tightly and placed in an oven at 120 °C for 24 hours. The mother solution was decanted and replaced with methanol and left at room temperature for 1 day. The crystals were collected by filtration then washed with methanol and dried at room temperature overnight.

*ZIF-8* crystals were synthesized by mixing  $\text{Zn}(\text{NO}_3)_2 \cdot 4\text{H}_2\text{O}$  (0.784 g) and 2-methylimidazole (0.492 g) in a 20 ml scintillation vial, before adding 10 ml of DMF to the mixture.<sup>3</sup> The mixture was stirred for few minutes to dissolve the reactants. The scintillation vial was capped tightly and placed in an oven at 100 °C for 2 days. Then the mother solution was decanted and replaced with 10 ml methanol and left at room temperature for 1 day. The crystals were collected by filtration then washed with methanol and dried at room temperature for overnight.

*ZIF-67* crystals were synthesized by mixing  $\text{Co}(\text{NO}_3)_2 \cdot 6\text{H}_2\text{O}$  (1.781 g) and 2-methylimidazole (0.995 g) in a 20 ml scintillation vial, before adding 15 ml of DMF to the mixture.<sup>4</sup> The mixture was stirred for few minutes to dissolve the reactants. The scintillation vial was capped tightly and placed in an oven at 125 °C for 2 days. The mother solution was decanted and replaced with 15 ml methanol and left at room temperature for 1 day. The crystals were collected by filtration then washed with methanol and dried at room temperature for overnight.

*UiO-66* was synthesised according to the procedure reported previously.<sup>5</sup> The product material was solvent exchanged overnight in methanol to replace any remaining N,N'-dimethylformamide (DMF) with methanol.

All the metal-organic framework materials were shown to be phase pure by powder X-ray diffraction.

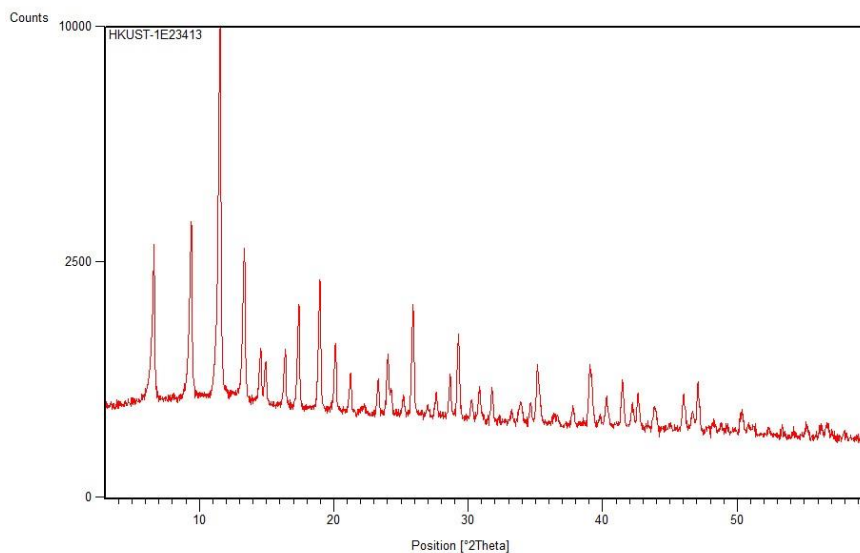


*Figure S8.* PXRD data for synthesized HKUST-1

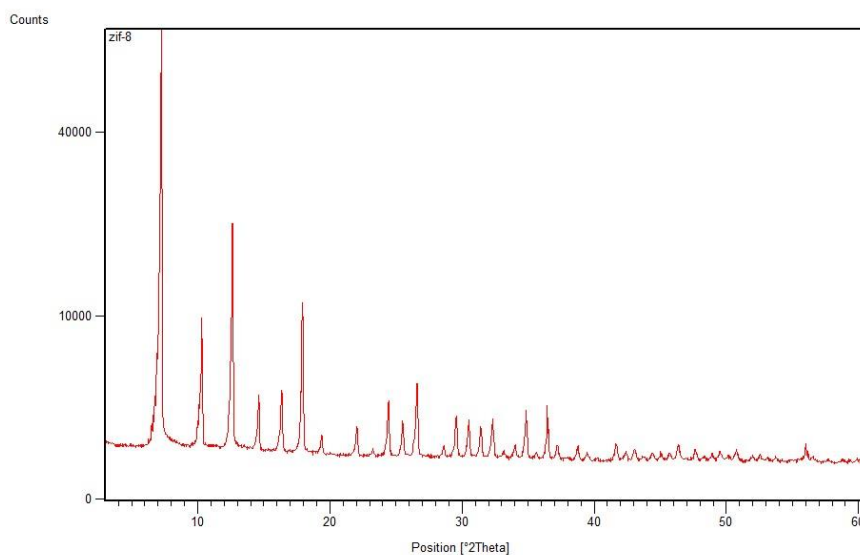


*Figure S9.* PXRD data for synthesized ZIF-8



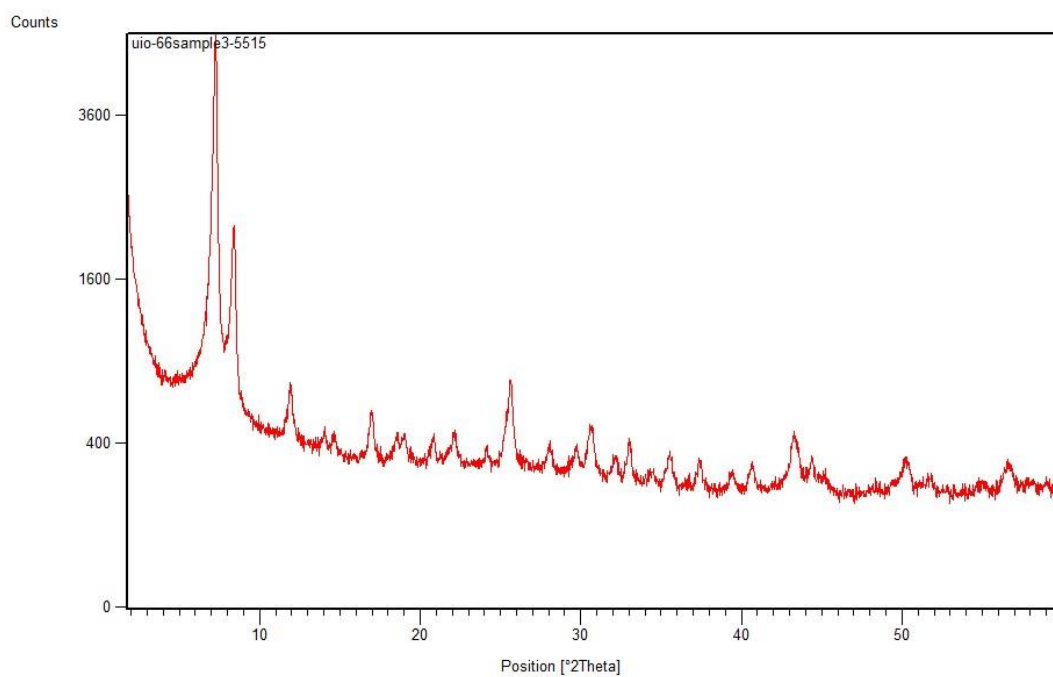


*Figure S10.* XRPD data for synthesized UiO-66

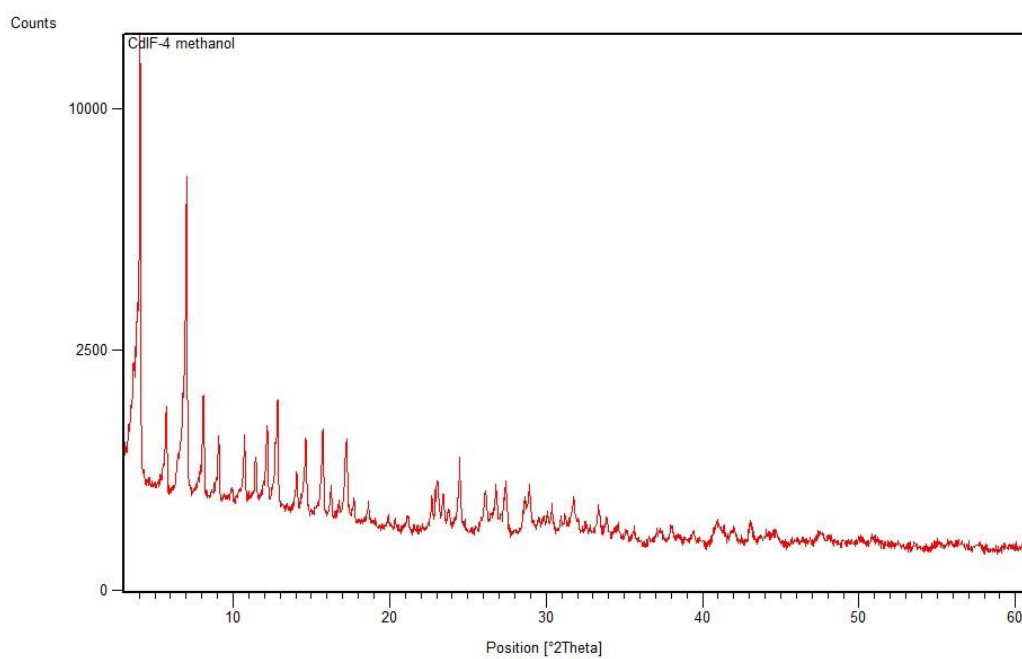


*Figure S11.* PXRD data for synthesized CdIF-4

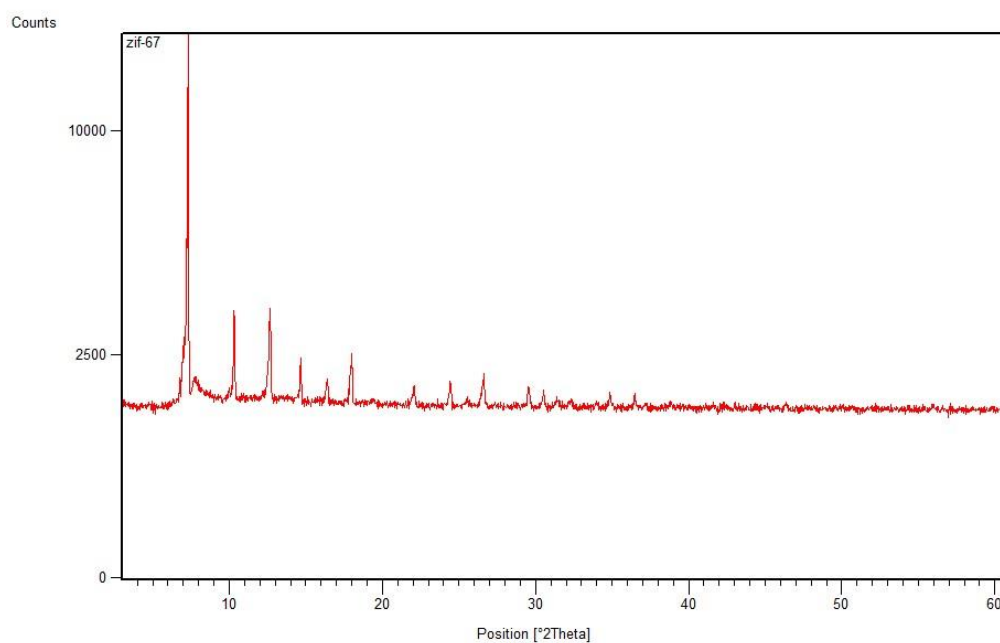


*Figure S12.* XRPD data for synthesized ZIF-67

## 7. Characterization of PIM-1

<i>M<sub>w</sub></i>	<i>M<sub>n</sub></i>	<i>M<sub>w</sub>/M<sub>n</sub></i>	<i>M<sub>p</sub></i>	<i>Solvent:Co-solvent</i>	<i>BET surface area (m<sup>2</sup>/g)</i>
128000	48800	2.62	87700	DMAc:Toluene (2:1)	705

## 8. Preparation and characterization of imprinted polymers

MIP microspheres were prepared by a suspension polymerization method according to our reported procedure.<sup>6</sup> In a typical MIP fabrication procedure the functional monomer (1 mmol), either NMP or DMF template (1 mmol), EDMA cross-linker (20 mmol), AIBN initiator (0.1 wt%), perfluoro polymeric surfactant (PFPS) emulsifier (100 mg), perfluoro methylcyclohexane (PMC) dispersing phase (80 mL) and acetonitrile porogen (15 mL) were stirred at a constant rotation rate of 300 rpm. The IPs were obtained by polymerization involving the irradiation of the stirred mixture with UV light for 6 hours at wavelength of 365 nm at room temperature under inert atmosphere. The resulting beads were filtered and the remaining template and unreacted molecules were extracted by sequential washing with methanol. The MIPs were dried under reduced pressure for 24 h at room temperature.

*Table S3.* Typical composition and stoichiometry for the imprinted polymers, where functional monomer FM1 is allylamine ( $pK_a = 9.53 \pm 0.29$ ), FM2 is 2-vinylpyridine ( $pK_a = 4.80 \pm 0.10$ ), FM3 is 1-vinylimidazole ( $pK_a = 6.07 \pm 0.10$ ), FM4 is acrylamide ( $pK_a = 15.35 \pm 0.50$ ), FM5 is N,N'-methylenebis(acrylamide) ( $pK_a = 13.07 \pm 0.46$ ), FM6 is methacrylic acid ( $pK_a = 4.58 \pm 0.11$ ), FM7 is 3-vinylphenylboronic acid ( $pK_a = 8.34 \pm 0.10$ ), and FM8 is itaconic acid ( $pK_a = 3.86 \pm 0.11$ ). High functional monomer/cross-linker ratio (1/20) was set resulting in highly cross-linked, robust polymeric networks.

	Template/Functional monomer/Crosslinker	T (mmol)	FM (mmol)	EDMA (mmol)	T (mg)	FM (mg)	EDMA (mg)	Porogen (mL)	PFPS (mg)	PMC (mL)	AIBN (mg)	IP (g)
MIP1	NMP/FM1/EDMA (1/1/20)	1	1	20	99.13	57.1	3964	15	100	80	4.0	4.02
MIP2	NMP/FM2/EDMA (1/1/20)	1	1	20	99.13	105.1	3964	15	100	80	4.1	4.07
MIP3	NMP/FM3/EDMA (1/1/20)	1	1	20	99.13	94.1	3964	15	100	80	4.1	4.06
MIP4	NMP/FM4/EDMA (1/1/20)	1	1	20	99.13	71.1	3964	15	100	80	4.0	4.04
MIP5	NMP/FM5/EDMA (1/1/20)	1	1	20	99.13	154.2	3964	15	100	80	4.1	4.12
MIP6	NMP/FM6/EDMA (1/1/20)	1	1	20	99.13	86.6	3964	15	100	80	4.1	4.05
MIP7	NMP/FM7/EDMA (1/1/20)	1	1	20	99.13	148.0	3964	15	100	80	4.1	4.11
MIP8	NMP/FM8/EDMA (1/1/20)	1	1	20	99.13	130.1	3964	15	100	80	4.1	4.09
MIP1	DMF/FM1/EDMA (1/1/20)	1	1	20	73.09	57.1	3964	15	100	80	4.0	4.02
MIP2	DMF/FM2/EDMA (1/1/20)	1	1	20	73.09	105.1	3964	15	100	80	4.1	4.07
MIP3	DMF/FM3/EDMA (1/1/20)	1	1	20	73.09	94.1	3964	15	100	80	4.1	4.06
MIP4	DMF/FM4/EDMA (1/1/20)	1	1	20	73.09	71.1	3964	15	100	80	4.0	4.04
MIP5	DMF/FM5/EDMA (1/1/20)	1	1	20	73.09	154.2	3964	15	100	80	4.1	4.12
MIP6	DMF/FM6/EDMA (1/1/20)	1	1	20	73.09	86.6	3964	15	100	80	4.1	4.05
MIP7	DMF/FM7/EDMA (1/1/20)	1	1	20	73.09	148.0	3964	15	100	80	4.1	4.11
MIP8	DMF/FM8/EDMA (1/1/20)	1	1	20	73.09	130.1	3964	15	100	80	4.1	4.09

Anal. Calcd/Found for extracted polymers: MIP1 for NMP (C, 60.64/60.59; H, 7.20/7.22; N, 0.37/0.35), MIP2 for NMP (C, 61.10/60.07; H, 7.11/7.08; N, 0.36/0.38), MIP3 for NMP (C, 60.68/60.64; H, 7.10/7.13; N, 0.71/0.67), MIP4 for NMP (C, 60.43/60.45; H, 7.12/7.15; N, 0.36/0.34), MIP5 for NMP (C, 60.38/60.41; H, 7.10/7.12; N, 0.70/0.73), MIP6 for NMP (C, 60.50/60.53; H, 7.12/7.15; N, 0.02/0.00), MIP7 for NMP (C, 60.76/60.74; H, 7.09/7.13; N, 0.02/0.00; B, 0.26/0.28), MIP8 for NMP (C, 60.14/60.17; H, 7.04/6.99; N, 0.02/0.04); MIP1 for DMF (C, 60.64/60.61; H, 7.20/7.18; N, 0.37/0.39), MIP2 for DMF (C, 61.10/60.05; H, 7.11/7.13; N, 0.36/0.33), MIP3 for DMF (C, 60.68/60.72; H, 7.10/7.06; N, 0.71/0.75), MIP4 for DMF (C, 60.43/60.46; H, 7.12/7.17; N, 0.36/0.32), MIP5 for DMF (C, 60.38/60.43; H, 7.10/7.14; N, 0.70/0.72), MIP6 for DMF (C, 60.50/60.46; H, 7.12/7.10; N, 0.02/0.03), MIP7 for DMF (C, 60.76/60.73; H, 7.09/7.12; N, 0.02/0.00; B, 0.26/0.24), MIP8 for DMF (C, 60.14/60.11; H, 7.04/7.07; N, 0.02/0.00). Elemental microanalysis of the polymers after extraction confirmed (i) the stoichiometrical incorporation of monomers into the polymers, and (ii) the successful removal of the template from the polymers.

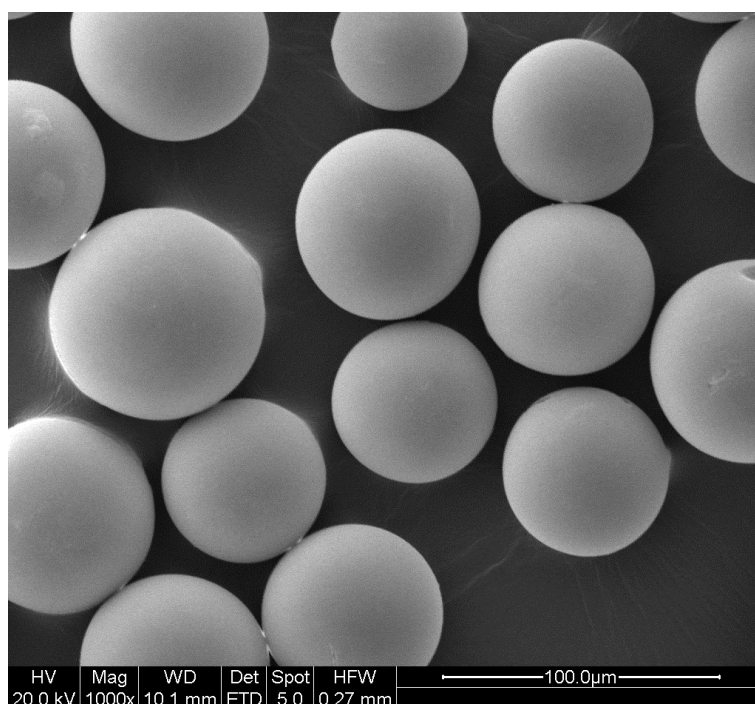


*Figure S13.* Typical scanning electron micrographs (SEM) of MIP7 imprinted polymer at 1000 magnification. The particles are spherical, uniformly sized with a size range of 40–80  $\mu\text{m}$ , which is suitable for chromatographic stationary phase and solid-phase extraction. BET analysis gave surface area of  $241 \text{ m}^2 \cdot \text{g}^{-1}$ , pore volume of  $0.114 \text{ cm}^3 \cdot \text{g}^{-1}$  and pore width of 1.89 nm.

## 9. Solvent flux decline of the membranes

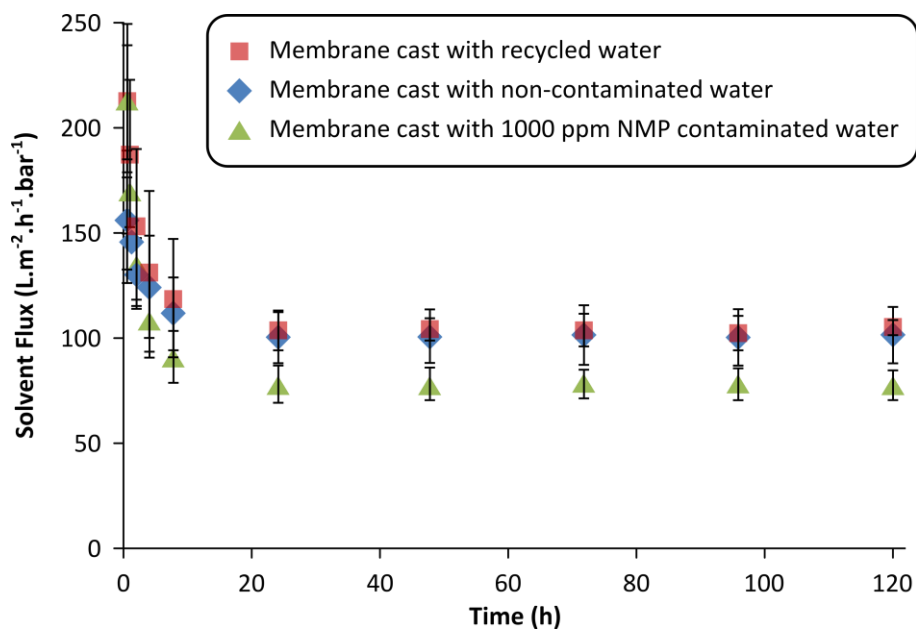


*Figure S14.* Flux decline data for the three different batches of membranes. Membranes prepared with NMP-containing wastewater exhibit lower flux and tighter rejection profile, whereas membranes prepared with treated and recycled wastewater showed identical performance compared to the prepared to the one prepared with fresh water, validating the recyclability of the purified water.

## 10. Calculation of Membrane Wastewater Generation

It can be calculated that 0.29 kg of dope (25 wt% polymer) is required to produce 1 m<sup>2</sup> of polymer membranes with 250 µm thickness. Note the polymer concentration does not affect the membrane production amount significantly. For instance, for 15 wt%, approximately 0.28 kg is required to produce 1 m<sup>2</sup> membranes.

From this calculation, the wastewater concentration can be estimated, as shown in *Figure 1* in the main text. Essentially, the wastewater concentration is determined by the coagulation bath size. Typically, the fabrication range is in between 100 – 500 L.m<sup>-2</sup>.

Hence, to produce a spiral-wound module with 40 m<sup>2</sup> membrane, approximately 4000 – 20,000 L of wastewater is generated.

Currently, about 500,000 spiral wound membrane module or 20 million m<sup>2</sup> membrane is fabricated solely for desalination each year, and subsequently 100-500 L.m<sup>-2</sup> wastewater is generated depending on the coagulation bath size.<sup>7</sup> Therefore, approximately 2 – 10 billion liters of wastewater are generated each year from desalination industry. Desalination is estimated to be only 1/5<sup>th</sup> of the entire membrane market and it is worth approximately \$1100 million.<sup>8</sup> Hence, it can be estimated that about 50 billion liters of wastewater is generated each year (*Figure S15*). Other significant membrane markets include the battery market which is approximately \$800 million,<sup>9</sup> the chloroalkyl process is also significant (market size could not be found), the gas separation market was \$150 million 10 years ago (likely to be much larger by now),<sup>10</sup> and most importantly, the artificial kidney market accounts for 50% of all the polymeric membranes produced.<sup>11</sup>

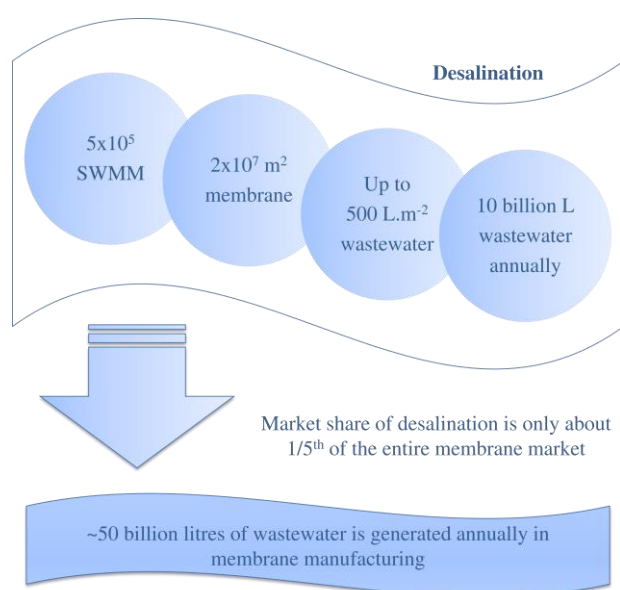


*Figure S15.* Estimation of the total wastewater generated by the membrane manufacturing industry.



## 11. Sustainability Assessment of Wastewater Treatment Process

### 11.1. Calculation of adsorbent mass

To calculate the required adsorbent mass to treat the wastewater, the two isotherm equations can be equated. Using MIP7 as an example which showed Redlich-Peterson isotherm behavior,

$$q_e = \frac{(C_o - C_e)m}{V} \quad \text{Eq. S14.}$$

$$q_e = \frac{K_R C_e}{1 + a_R C_e^g} \quad \text{Eq. S15.}$$

$$\frac{(C_o - C_e)m}{V} = \frac{K_R C_e}{1 + a_R C_e^g} \quad \text{Eq. S16.}$$

where  $C_o$  and  $C_e$  are the initial and equilibrium concentrations of the solution, respectively,  $m$  represents the adsorbent mass,  $V$  refers to the system volume, and  $K_R$ ,  $a_R$ , and  $g$  represent the model constants.

Solving for  $m$  yields the following equation,

$$m = \frac{K_R C_e}{1 + a_R C_e^g} \times \frac{V}{(C_o - C_e)} \quad \text{Eq. S17.}$$

Hence, the required adsorbent mass,  $m$ , can be calculated by defining the final wastewater concentration. In our work, the allowable concentration limit is 100 ppm.

### 11.2. Calculation of Process Mass Intensity

The mass intensity can be calculated using Eq. 1 in the main text. The mass intensity of membrane fabrication without adsorbent is simply the sum of the dope mass and water mass. The mass intensity of membrane fabrication with the adsorbent unit is the sum of dope mass, the required adsorbent mass, and the washing solvent for adsorbent regeneration. The water mass is not included as it is assumed to be recycled.

### 11.3. Adsorbent Recovery Calculation

To calculate the energy requirement for solvent regeneration, the pump energy and desorption energy were calculated. To calculate the pump energy, the pressure difference was assumed to be 2 bar and the required washing solvent was 4 L.m<sup>-2</sup>. The desorption energy was assumed to be 4.2 KJ.kg<sup>-1</sup> of NMP.

To calculate the energy requirement for vacuum regeneration, the required vacuum energy and the evaporation energy were calculated. To calculate the vacuum energy, the volume was taken as the column dimension (10 x 250 mm) and the vacuum pressure was to be 0.01 mbar. The evaporation energy at ambient temperature was calculated using the latent heat of evaporation of 510.4 KJ.kg<sup>-1</sup>.

To calculate the thermal regeneration energy, the heating energy and the evaporation energy were calculated. The energy required to heat the adsorbent up to 1000 oC was calculated using an charcoal heat capacity value of 1500 J.kg<sup>-1</sup>.K<sup>-1</sup>. The evaporation energy calculation was the same as before.

Approximately 1.67 Kg MIP7 adsorbent is required to purify 221 Kg wastewater (contaminated with 1000 ppm solvent) and it requires approximately 5 L and 4 L of solvent to prepare and regenerate 1 kg of MIP7 adsorbent, respectively. Hence, the purified wastewater to generated waste ratio can be calculated as shown in *Figure S16*. Given the robust nature of imprinted polymers due to high crosslinking degree, they can be regenerated about 50 times,<sup>12</sup> maximizing the ratio up to 54 Kg.Kg<sup>-1</sup>.

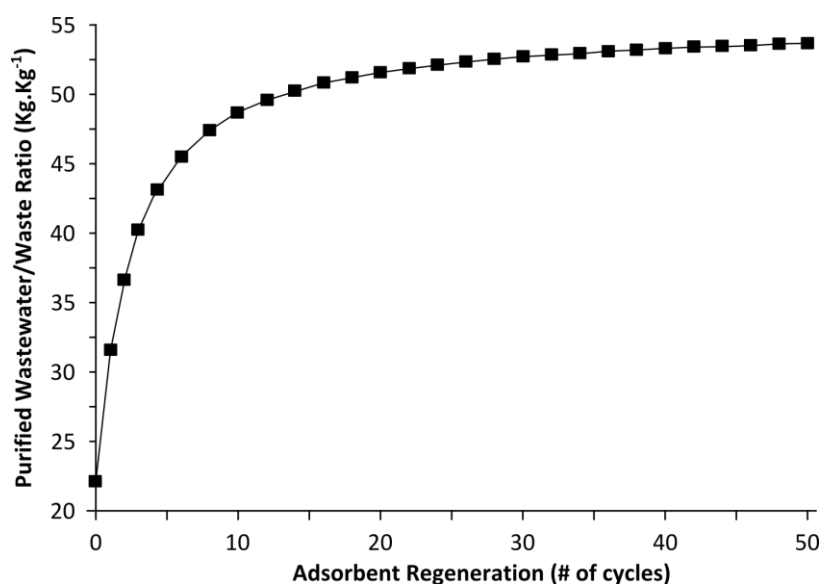


*Figure S16.* Ratio of purified wastewater to waste generated. Waste includes the discharged adsorbent as well as the waste solvent generated during MIP7 adsorbent preparation and regeneration.

### 11.4. Process Energy Calculation

To calculate the energy requirement for single-pass distillation, the heating energy, the evaporation energy, the condensation energy, and the cooling energy were calculated (*Table S4*). The heat capacity of the NMP was  $4.2 \text{ J.g}^{-1}.\text{K}^{-1}$ .

*Table S4. Distillation Calculation (Concise Version).*

Water Volume (m <sup>3</sup> )	Volume-Area (L.m <sup>-2</sup> )	Solvent Concentration (g.L <sup>-1</sup> )	Heating to BP (kJ)	Evaporation (KJ)	Condensation (KJ)	Cooling to RT (KJ)	Distillation Total Energy (kJ)
5	14.75	67.8	4646	33314	33314	4646	75921
50	147.49	6.78	46460	333145	333145	46460	759210
100	294.99	3.39	92920	666290	666290	92920	1518420
110	324.48	3.08	102212	732919	732919	102212	1670262
120	353.98	2.83	111504	799548	799548	111504	1822104

The pervaporation energy was calculated by summing up the heating energy to 70 °C, evaporation & condensation energies for water and NMP, and the cooling energy (*Table S5*). It was assumed equi-volume of NMP and water permeated through an arbitrary pervaporation membrane.

*Table S5. Pervaporation calculations.*

Water Volume (m <sup>3</sup> )	Volume-Area (L.m <sup>-2</sup> )	Solvent Concentration (g.L <sup>-1</sup> )	Heating to 70°C (KJ)	Heat of Vaporization (NMP) (KJ)	Heat of Vaporization (Water) (KJ)	Heat of Condensation (both) (KJ)	Cooling (KJ)	Pervaporation Total (KJ)
5	14.75	67.8	2788	451	2259	2710	2788	10995
50	147.49	6.78	27876	451	2259	2710	27876	61172
100	294.99	3.39	55752	451	2259	2710	55752	116924
110	324.48	3.08	61327	451	2259	2710	61327	128074
120	353.98	2.83	66903	451	2259	2710	66903	139225

The adsorption energy was calculated to operate isothermal adsorption process (*Table S6*). The employed heat of adsorption was  $60.7 \text{ KJ.mol}^{-1}$ .

*Table S6. Adsorption calculations.*

Water Volume (m <sup>3</sup> )	Volume-Area (L.m <sup>-2</sup> )	Solvent Concentration (g.L <sup>-1</sup> )	Pump Energy (2 bar)	Heat of Adsorption (KJ)	Required Cooling (KJ)	Adsorption Total Energy (KJ)
5	14.75	67.8	3.0	612.0	612.0	1227.0
50	147.49	6.78	29.9	612.0	612.0	1253.9
100	294.99	3.39	59.8	612.0	612.0	1283.8
110	324.48	3.08	65.8	612.0	612.0	1289.8
120	353.98	2.83	71.7	612.0	612.0	1295.7

## References

- <sup>1</sup> S. S. Y. Chiu, S. M. F. Lo, J. P. H. Charmant, A. G. Orpen, I. D. Williams, *Science*, 1999, **283**, 1148–1150.
- <sup>2</sup> Y. Q. Tian, S. Y. Yao, D. Gu, K. H. Cui, D. W. Guo, G. Zhang, Z. X. Chen, D. Y. Zhao, *Chem. Eur. J.*, 2010, **16**, 1137–1141.
- <sup>3</sup> X. C. Huang, Y. Y. Lin, J. P. Zhang, X. M. Chen, *Angew. Chem. Int. Ed.*, 2006, **45**, 1557–1559.
- <sup>4</sup> R. Banerjee, A. Phan, B. Wang, C. Knobler, H. Furukawa, M. O’Keeffe, O. M. Yaghi, *Science*, 2008, **319**, 939–943.
- <sup>5</sup> J. H. Cavka, S. Jakobsen, U. Olsbye, N. Guillou, C. Lamberti, S. Bordiga, K. P. Lillerud, *J. Am. Chem. Soc.*, 2008, **130**, 13850–13851.
- <sup>6</sup> J. Kupai, E. Rojik, P. Huszthy, G. Szekely, *ACS Appl. Mater. Interfaces*, 2015, **7**, 9516–9525.
- <sup>7</sup> T. Fane, TCE, July 2013
- <sup>8</sup> Global Water Intelligence Report, Volume 49, Issue 18, 2013
- <sup>9</sup> Yano Research Institute, 2012, Lithium ion battery material market perspective – four key materials (C54104000).
- <sup>10</sup> R. W. Baker, *Ind. Eng. Chem. Res.*, 2002, **41**, 1393–1411.
- <sup>11</sup> R. W. Baker Ed., *Membrane Technology and Applications*, Chapter 12, Wiley, 2012
- <sup>12</sup> B. Sellergren, *Molecularly Imprinted Polymers: Man-made Mimics of Antibodies and their Applications in Analytical Chemistry*, 1st ed., Elsevier, Amsterdam, 2001.